FEATURE ARTICLE

Electronic Excitation Transport in Disordered Finite Volume Systems

M. D. Ediger[†] and M. D. Fayer*

Department of Chemistry, Stanford University, Stanford, California 94305 *(Received: August 16, 1984)*

An account of recent theoretical and experimental advances in the field of excitation transport in disordered finite volume systems is presented. A theoretical approach is described which demonstrates that the spatial extent of a system of chromophores can have a profound effect on excitation transport. Experiments on a finite volume system, octadecyl rhodamine B in micelles, are described. This clustered transport system is shown to be highly efficient. Theoretical analysis permits the determination of the size of the micelle. The finite volume theory is then adapted to describe excitation transfer among chromophores attached to an isolated polymer coil or small aggregate of coils in a polymer blend. It is shown that information about polymer configurations can be obtained from excitation transport experiments. Experimental measurements on excitation transfer between a pair of chlorophyll molecules substituted into hemoglobin are described. These experiments yield an absolute determination of the direction of the chlorophyll transition dipole relative to the molecular axis system.

I. Introduction

In recent years considerable progress has been made in the study of electronic excitation transport processes in a variety of condensed-phase systems. This collisionless, nonradiative resonance transfer process was first described in quantum mechanical terms by Förster over 30 years ago.[1] Since then, work in many scientific fields has revealed the ubiquitous nature of electronic excitation transfer. It is involved in concentration quenching of fluorescence in solution[2-5] as well as in sensitized luminescence in gases,[2] liquids,[6,7] and solids.[8] Excitation transport is a critical step in the primary stages of photosynthesis[9] and is also responsible for time-dependent emission line shape effects in mixed molecular crystals[10] and glasses.[11]

Excitation transfer between molecules occurs because of intermolecular interactions, e.g., multipolar or exchange, which couple the states of the molecules.[1,12] For all the experimental systems described in this paper, the intermolecular interaction energy is much smaller than fluctuations in the molecular energy levels caused by rapid thermal motions of the medium. In this case, the excitation transport process is incoherent[13] and can be described in classical terms; only excitation probabilities need be considered. Therefore, a theoretical treatment based on the master equation can be employed.

[†] Permanent address: Department of Chemistry, University of Wisconsin, Madison, WI 53706.

(1) Th. Förster, *Ann. Phys. Leipzig*, **2**, 860 (1948); **2**, 55 (1948); *Z. Naturforsch. A*, **4**, 321 (1949).
(2) R. Livingston, *J. Phys Chem.*, **61**, 860 (1957).
(3) D. R. Lutz, K. A. Nelson, C. R. Gochanour, and M. D. Fayer, *Chem. Phys.*, **58**, 325 (1981).
(4) M. D. Fayer, *Annu. Rev. Phys. Chem.*, **33**, 63 (1982).
(5) F. P. Schäfer, In "Topics in Applied Physics", 2nd ed. Vol. 1, F. P. Schäfer, Ed., Springer-Verlag, New York, 1977, pp 21–24, 158–60.
(6) Th. Förster, *Z. Elektrochem.*, **53**, 93 (1949).
(7) R. J. D. Miller, M. Pierre, and M. D. Fayer, *J. Chem. Phys.*, **78**, 5138 (1983).
(8) S. T. Gentry and R. Kopelman, *J. Chem. Phys.*, **78**, 373 (1983); S. T. Gentry, Ph.D. Thesis, University of Michigan, Ann Arbor, MI, 1983.
(9) Kenneth Sauer, *Acc. Chem. Res.*, **7**, 257 (1978).
(10) Jack R. Morgan and M. A. El Sayad, *J. Phys. Chem.*, **87**, 2178 (1983).
(11) M. J. Weber In "Topics in Applied Physics", Vol. 49, W. M. Yen and P. M. Selzer, Ed., Springer-Verlag, New York, 1981, pp 189–240.
(12) D. L. Dexter, *J. Chem. Phys.*, **21**, 836 (1953); M. Inokuti and F. Hirayama, *J. Chem. Phys.*, **43**, 1978 (1965).

0022-3654/84/2088-6108$01.50/0

Since the coupling between molecules is strongly distance dependent, the excitation transfer rate is as well.[1] For molecules distributed randomly within some volume, the large distribution of intermolecular distances implies a large distribution of transfer rates. The mathematical treatment of such problems involves very large systems of coupled linear differential equations (the master equation) which cannot be solved exactly. In the past few years, rapid progress has been made in developing accurate nonperturbative approximations for this kind of problem in systems large enough to be taken as infinite in extent.

The nature of excitation transport among chromophores (donors) distributed randomly in an infinite solution has been studied extensively. This is a classic problem treated by Förster over 30 years ago.[1] Förster simplified the complex problem of the disordered system by taking the donors to be equally spaced at the average spacing for a given donor concentration. Excitation transport within this approximation was shown to be diffusive at long times, i.e., the mean-square displacement of the excitation increases linearly in time. However, work in the past few years has shown that this is not an accurate descritpion of excitation transport dynamics. Transport is not diffusive.[14,15] Picosecond fluorescence mixing experiments[17] on rhodamine 6G in solution demonstrate that recent theoretical advances provide an accurate and comprehensive description of excitation transport among randomly distributed donors in an infinite solution. The new theory employs a diagrammatic approach to the solution of the master equation for this problem.[15] This approach is very powerful and has been extended to other problems.[18a-c,19,20]

Transport and trapping in an infinite solution has also been considered. Trapping of electronic excitations is responsible for phenomena such as sensitized luminescence in crystals and solutions[12] and sensitized photochemistry such as photosynthesis.[9] The study of transport and trapping dynamics has become an important tool for investigating biological[21] and polymer systems.[22] Förster considered excitation transport in solutions containing two solute species: donor molecules and traps molecules. An electronic excitation could be transferred from donor to trap via a resonant dipole–dipole interaction. (Subsequently the work was extended to higher multipole and exchange interactions.[12]) Förster treated the case in which the trap concentration is much greater than the donor concentration. Each donor is assumed to interact only with an ensemble of neighboring traps so transport from one donor to another is neglected. Neglect of donor–donor transport greatly simplifies the theoretical problem.

By applying the diagrammatic technique developed for the donor-to-donor transport problem to donor–trap systems,[18a] it has been possible to obtain an accurate description of excitation transport dynamics for any concentration of donors and traps.[7] Picosecond fluorescence mixing and transient grating experiments were employed to examine transport and trapping in solutions with a wide range of donor and trap concentrations.[3,4,7] Comparisons of experiment and theory demonstrate that we have a comprehensive understanding of this type of system. (The general problem of donor-to-donor transport prior to trapping can be handled for any form of the intermolecular interaction distance dependence. While electronic excitations are being discussed here, the theoretical results apply to electron transport as well.)

The random solution theory for transport and trapping of excitations has been extended to the case of molecules randomly substituted on an infinite lattice.[18b-d] In the lattice theory, the distance variable is no longer continuous. It is necessary to exclude configurations in which two molecules are on the same lattice site when performing ensemble averages over the possible positions of all particles. This greatly increases the complexity of the problem. The diagrammatic theory for the lattice problem allows accurate results to be obtained from low concentration to a filled lattice.

In this article we focus our attention on recent theoretical and experimental studies of excitation transport in finite volume systems. There are a variety of interesting systems in which chromophores are contained in a volume sufficiently small that energy transport properties are significantly affected by the limited size of the system.[22] Such finite volume systems include isolated polymer coils containing chromophores,[23-25] small aggregates of coils in polymer blends,[25] micelles containing dye molecules,[26-28] and photosynthetic units.[9829,30]

Constraining chromophores to a finite volume increases the theoretical complexity of the excitation transport problem.[23] For an infinite volume system, the ensemble-averaged Green function solution to the master equation is independent of the initial position of the excitation.[15] This property allows a very accurate approximation to be obtained by nonperturbative techniques. In contrast, a chromophore near the surface of a finite sphere of randomly distributed chromophores experiences a very different local distribution of chromophores than a chromophore near the center. Therefore, an additional average over the excitation starting point must be performed. The finite volume theory must also be able to handle finite numbers of particles. These differences from the infinite volume problem make the nonperturbative theoretical techniques inapplicable to finite volume systems. Instead a density expansion with a Padé approximant is used. These theoretical results have been shown to be accurate.[23,26]

As an example of excitation transfer in a finite volume system, picosecond fluorescence mixing experiments on octadecyl rhodamine B (ODRB) in Triton X-100 micelles are described.[26] The ODRB is insoluble in water and is totally associated with the micelles. ODRB in micelles forms a clustered energy transport system. By clustering the dye molecules in a small volume, the transport efficiency is greatly increased over a solution with the same dye concentration but with the molecules randomly distributed throughout the solution. Very rapid energy transport is observed and agreement with theory is very good. The experiments provide an accurate determination of the micelle size.

The finite volume excitation transport theory is then applied to isolated polymer coils and small aggregates of coils, for polymers that contain chromophores.[25] Examples of common polymers containing chromophores are polystyrene and polyvinyl-

(13) See articles in "Spectroscopy and Excitation Dynamics of Condensed Molecular System", V. M. Agranovich and R. M. Hochstrasser, Ed., North-Holland, New York, 1983.

(14) S. W. Haan and R. Zwanzig, *J. Chem. Phys.*, **68**, 1879 (1978).

(15) C. R. Gochanour, H. C. Andersen, and M. D. Fayer, *J. Chem. Phys.*, **70**, 4254 (1979).

(16) J. Klafter and R. Silbey, *J. Chem. Phys.*, **72**, 843 (1980); K. Godzik and J. Jortner, *ibid.*, **72**, 4471 (1980); B. Movaghar and G. W. Sauer, *J. Phys. C*, **13**, 4933 (1980).

(17) C. R. Gochanour and M. D. Fayer, *J. Phys. Chem.*, **85**, 1989 (1981).

(18) (a) R. F. Loring, H. C. Andersen, and M. D. Fayer, *J. Chem. Phys.*, **76**, 2015 (1982); **77**, 1079(E) (1982); (b) R. F. Loring, H. C. Andersen, and M. D. Fayer, *Phys. Rev. Lett.*, **50**, 1324 (1983); **51**, 718(E) (1983); R. F. Loring, H. C. Andersen, and M. D. Fayer, *J. Chem. Phys.*, **80**, 5731 (1984); (c) R. F. Loring, H. C. Andersen, and M. D. Fayer, *Chem. Phys.*, **85**, 149 (1984); (d) T. Odagaki and M. Lax, *Phys. Rev. B*, **24**, 5284 (1981); G. Korzeniewski, R. Friesner, and R. Silbey, *J. Stat. Phys.*, **31**, 451 (1983).

(19) G. H. Fredrickson, H. C. Andersen, and C. W. Frank, *Macromolecules*, **16**, 1456 (1983); **17**, 54 (1984); *J. Chem. Phys.*, **79**, 3572 (1983).

(20) R. Parson, *Chem. Phys. Lett.*, **100**, 59 (1983).

(21) R. E. Dale and J. Eisinger, *Proc. Natl. Acad. Sci. U.S.A.*, **73**, 271 (1976).

(22) C. W. Frank, M. A. Gashgari, P. Chutikamontham, and V. J. Haverly in "Studies in Physical and Theoretical Chemistry", Vol. 10, A. G. Walton, Ed., Elseview, Amsterdam, 1980, pp 187–209; W. Klöpffer, *Ann. N.Y. Acad. Sci.*, **366**, 373 (1981).

(23) M. D. Ediger and M. D. Fayer, *J. Chem. Phys.*, **78**, 2518 (1983).

(24) M. D. Ediger, R. P. Domingue, K. A. Peterson, and M. D. Fayer, *Macromolecules*, accepted for publication.

(25) M. D. Ediger and M. D. Fayer, *Macromolecules*, **16**, 1839 (1983).

(26) M. D. Ediger, R. P. Domingue, and M. D. Fayer, *J. Chem. Phys.*, **80**, 1246 (1984).

(27) G. A. Kenney-Wallace, J. H. Flint, and Stephen C. Wallace, *Chem. Phys. Lett.*, **32**, 71 (1975).

(28) Peter K. F. Koglin, Dennis J. Miller, Jürgen Steinwandel, and Manfred Hauser, *J. Phys. Chem.*, **85**, 2363 (1981).

(29) R. S. Moog, A. Kuki, M. D. Fayer, and S. G. Boxer, *Biochemistry*, **23**, 1564 (1984).

(30) G. S. Beddard and G. Porter, *Nature (London)*, **260**, 366 (1976).

naphthalene. Due to the strong distance dependence of the transfer rate, the dynamics of excitation transport in a finite volume are intimately related to the average interchromophore separation, and hence the overall size of the chromophore distribution. Excitation transport observables can serve as a tool for examining the spatial configuration of polymer coils just as these observables allowed the determination of the Triton micelle size.[26] Of particular interest is how coil size changes in various polymer blends. The experimental results presented here indicate that the finite volume theory correctly describes the time dependence of excitation transport in an isolated polymer coil.[24]

Like micelles or polymers, the natural photosynthetic unit is a finite volume energy transport system; plants take advantage of the efficiency of a clustered transport system to move optical excitations from the absorbing chlorophylls to the photosynthetic reaction center.[9,30] The relationship between structure and function of the photosynthetic unit is a problem on which tremendous research effort is being expended. The orientation of the chlorophyll transition dipole is the cornerstone of all interpretations of polarized light spectroscopy, excitonic interactions, and resonant excitation transfer in natural chlorophyll-containing systems. Recently the transition dipole orientation was determined by examining excitation transport between two chlorophyll molecules in a synthetic chlorophyllide substituted hemoglobin.[29]

The phenomenon of hopping transport in disordered systems is of considerable interest in many areas of solid-state physics, chemistry, and biology. An understanding of the pairwise interactions which cause excitation transport, coupled with an appropriate theoretical approach, allows detailed information about molecular properties and the properties of large assemblies of molecules to be extracted from experimental investigations.

II. Theory

An important characteristic of a disordered system is the statistical distribution of intermolecular distances, which leads to a distribution of transfer rates from an initially excited molecule to surrounding unexcited molecules. There is not a single path by which excitation probability is transferred between two molecules but rather a very large set of possible paths involving all the molecules in the sample. An ensemble average over this set of paths is necessary to describe the actual transfer process. Qualitatively, it is not difficult to appreciate the effects of the finite volume on the problem. Molecules near the edge of the volume have a smaller number of nearby chromophores than molecules near the center. Thus, the time required for transport away from the originally excited molecule averaged over all starting positions and chromophore configurations in the finite volume will be slower than in an infinite volume of the same chromophore density. Additionally, transport cannot become diffusive in the long time limit even in the absence of traps. The mean-squared displacement must approach a constant as excitation probability is equalized throughout the finite volume. Clearly, the effects of the finite volume will be most pronounced when the volume dimensions are comparable to the critical radius for energy transport R_0. Finite volumes significantly alter the behavior of time-dependent observables in many cases.[23]

Each configuration of N molecules distributed randomly in a volume Ω is characterized by the location and orientation of the N molecules $(\mathbf{r}_1,\psi_1;\mathbf{r}_2,\psi_2;\ldots;\mathbf{r}_N,\psi_N)$. The vector $\mathbf{r}_i$ gives the location of molecule i while ψ_i represents the set of angular coordinates necessary to specify the orientation of the transition dipole. The master equation for each configuration, denoted by R, is

$$dp_j(R,t)/dt = -p_j(R,t)/\tau + \sum_k w_{jk}[p_k(R,t) - p_j(R,t)] \quad (1)$$

where $p_j(R,t)$ is the probability that an excitation is found on molecule j in configuration R at time t, τ is the measured lifetime, and w_{jk} is the transfer rate between molecule j and k. For dipole–dipole interactions, the transfer rate is

$$w_{jk} = \tfrac{3}{2}\tau^{-1}K_{jk}^2(R_0/r_{jk})^6 \quad (2)$$

R_0 characterizes the strength of the intermolecular interaction and can be determined from steady-state spectroscopy.[1] Qualitatively, R_0 is a measure of the distance over which energy transport is efficient in comparison to lifetime processes. The orientation factor K_{jk}^2 is dependent on the relative orientation of the transition dipoles of molecules j and k and can be written as

$$K_{jk}^2 = [\hat{\mathbf{d}}_j\cdot\hat{\mathbf{d}}_k - 3(\hat{\mathbf{d}}_j\cdot\hat{\mathbf{r}}_{jk})(\hat{\mathbf{d}}_k\cdot\hat{\mathbf{r}}_{jk})]^2 \quad (3)$$

where $\hat{\mathbf{d}}_j$ and $\hat{\mathbf{d}}_k$ are unit vectors in the directions of the transition dipoles of molecules j and k and $\hat{\mathbf{r}}_{jk}$ is a unit vector in the direction of a vector connecting molecule j and k.

The quantity most useful for obtaining information concerning transport is the Green function:

$$G(\mathbf{r},\mathbf{r}',t) = G^s(\mathbf{r}',t) + G^m(\mathbf{r},\mathbf{r}',t) \quad (4)$$

The Green function can be thought of as the probability of finding an excitation at position $\mathbf{r}$ and time t with the initial condition of unit probability at $\mathbf{r}'$. It is convenient to divide the Green function into two terms, one which is a measure of probability at the initial site of excitation $\mathbf{r}'$, $G^s(\mathbf{r}',t)$ and one which is a measure of the probability found on a molecule a distance $\mathbf{r}-\mathbf{r}'$ from the initial site, $G^m(\mathbf{r},\mathbf{r}',t)$.

As discussed in the Introduction, this problem cannot be solved exactly. We have employed an expansion in powers of the chromophore density to investigate the finite volume problem.[23] It provides results that are most accurate for short times or low concentrations. For certain properties, such as the probability of finding an excitation on the originally excited molecule ($G^s(t)$), the density expansion can provide a very good approximation for all experimentally accessible times.

The Laplace transform of $G^s(t)$ can be written in powers of the chromophore density as

$$\hat{G}^s(N,\Omega,\mathbf{r},\mathbf{r}',\epsilon) = 1/\epsilon - \frac{N-1}{\Omega}B_2(\Omega,\mathbf{r},\mathbf{r}',\epsilon) - \frac{(N-1)(N-2)}{\Omega^2}B_3(\Omega,\mathbf{r},\mathbf{r}',\epsilon) - \ldots \quad (5)$$

Here Ω characterizes the volume containing the chromophores. The term B_2 contains information about two-particle interactions. Similarly, B_n contains information about n-particle interactions. If a general expression for the nth term could be found, $\hat{G}^s(\epsilon)$ could be calculated exactly. In practice, only the first two terms can usually be evaluated. Since we are interested in situations where the chromophores are randomly distributed within the finite volume, we need to ensemble average the above expression over all possible chromophore positions. The truncated density expansion for an orientation averaged transfer rate[26] then yields eq 6 where explicit expressions have been used for B_2 and B_3.

$$\hat{G}^s(N,\Omega,\epsilon) = \frac{1}{\epsilon} - \frac{(N-1)}{\Omega^2}\int_\Omega d\mathbf{r}_1\int_\Omega d\mathbf{r}_2\,\frac{w_{12}}{\epsilon(\epsilon+2w_{12})} - \frac{(N-1)(N-2)}{\Omega^3}\int_\Omega d\mathbf{r}_1\int_\Omega d\mathbf{r}_2\int_\Omega d\mathbf{r}_3 \left\{\frac{\epsilon w_{12} + w_{12}w_{13} + w_{12}w_{23} + w_{13}w_{23}}{\epsilon[\epsilon^2 + 2\epsilon(w_{12}+w_{13}+w_{23}) + 3(w_{12}w_{13}+w_{12}w_{23}+w_{13}w_{23})]} - \frac{w_{12}}{\epsilon(\epsilon+2w_{12})}\right\} \quad (6)$$

Equation 6 is the exact solution to the finite volume problem for three or fewer particles. It is a reasonable but not very good approximation for larger numbers of particles. We obtain a better approximation for $\hat{G}^s(\epsilon)$ by using the Padē approximant

$$\hat{G}^s(N,\Omega,\epsilon) = \epsilon^{-1}\{1 + (N-1)\epsilon h_2 + (N-1)[(N-1)(\epsilon h_2)^2 - (N-2)\epsilon h_3]\}^{-1} \quad (7)$$

Here h_2 and h_3 represent the two- and three-particle integrals in eq 6. h_2 and h_3 are functions of Ω, ϵ, and the transfer rate.

Padé approximants are frequently used in statistical mechanics to approximate truncated power series expansions such as eq 6.[32] No matter how many terms were calculated in the expansion for $\hat{G}^s(N,\Omega,\epsilon)$, the result would be ill behaved for large N or small ϵ. Equation 7, in contrast, shows the proper asymptotic behavior in these limits and is a very good approximation to $\hat{G}^s(N,\Omega,\epsilon)$.

The relationship between the inverse Laplace transform of $\hat{G}^s(N,\Omega,\epsilon)$, $G^s(N,\Omega,t)$, and the results of a fluorescence depolarization experiment is easily understood. If chromophores in a viscous medium are irradiated with a short pulse of polarized light, molecules with their transition dipoles oriented parallel to the excitation polarization are preferentially excited. If the ensuing fluorescence is detected through a polarizer, the initial ratio of parallel polarized fluorescence intensity to perpendicular polarized intensity is about 3:1. In a low concentration sample where energy transfer does not occur, both components of the fluorecence decay with the lifetime and the polarization ratio is preserved. In higher concentration samples excited-state population is transferred to molecules with a range of orientations, and the fluorescence becomes depolarized. Galanin has shown that the overwhelming contribution to fluorescence polarization is due to fluorescence from chromophores which were initially excited,[33,34] i.e., energy transfer can be taken to occur to a randomly oriented chromophore. Thus the time dependence of fluorescence depolarization will be directly related to the fundamental property which characterizes energy transport, the time-dependent probability that the excitation is at the initial site, $G^s(t)$.

III. Experimental Methods

The experiments presented in sections IV and VI were performed with the fluorescence mixing technique. In these experiments, a specific polarization component of the fluorescence decay is directly observed. The setup shown in Figure 1 is configured for the experiments on excitation transport among dye molecules in micelles[26] (section IV). The laser is a continuously pumped Nd:YAG system which is acousto-optically Q-switched and mode-locked to produce trains of about 40 pulses at 1.06 μm, with 1.3 mJ per pulse train. The YAG pulse train is frequency doubled and used to synchronously pump a dye laser which is spectrally narrowed and tuned by two intracavity etalons. The dye laser is cavity dumped by a Pockels cell with avalanche transistor driver to give a 20-μJ, 30-ps pulse with a spectral width of 1 cm^{-1}. A dye laser single pulse at 562 nm excites the sample. The resulting fluorescence is filtered to removed scattered excitation light and focused into an RDP type-I sum-generating crystal where it overlaps with the path of a 1.06-μm single pulse selected from the YAG laser pulse train by a Pockels cell and polarizer. The fluorescence reaching the sum crystal coincident in time with the 1.06-μm pulse mixes with that pulse to produce a short burst of UV light (~380 nm). The UV intensity is proportional to the fluorescence intensity at that time. The sum crystal is oriented so that only the component of the fluorescence polarized parallel to the 1.06-μm polarization is summed. A half-wave plate varies the polarization of the excitation pulse relative to the summing pulse, allowing both the parallel and perpendicular polarization components of the fluorescence ($I_\parallel(t)$ and $I_\perp(t)$) to be obtained. The excited-state lifetime can be determined directly by adjusting the relative polarization of the excitation and summing pulses to the magic angle (54.7°).[17] At this angle a signal proportional to the total fluorescence is obtained, i.e., depolarization processes do not contribute to the signal.

The time decay is swept out by varying the delay between the excitation pulse and the summing pulse with a motorized delay line. The signal is detected through a UV bandpass filter by a cooled photomultiplier. The phototube output is measured with a lock-in amplifier operating at the laser frequency. The lock-in output and a voltage proportional to the delay time are digitized and stored on disk.

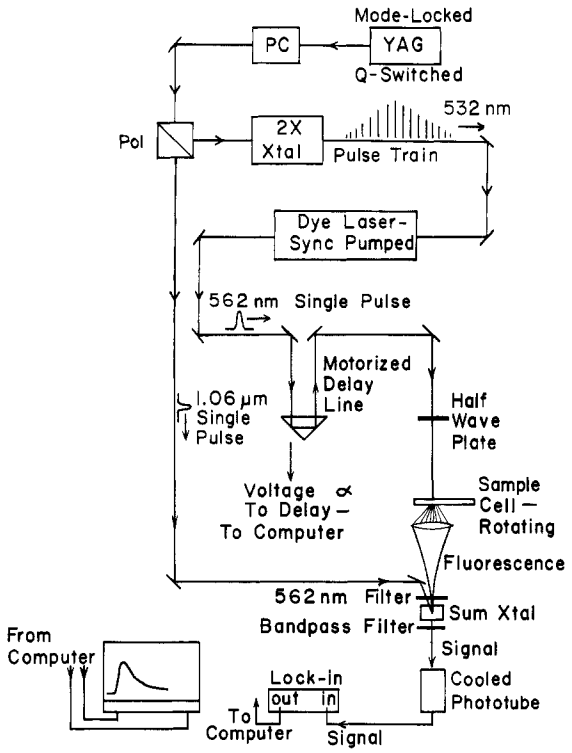

Figure 1. Fluorescence mixing experimental setup: PC = Pockels cell; Pol = polarizer. The sample is excited by a variably delayed dye laser pulse. The resulting fluorescence is summed with a 1.06-μm pulse which provides the time resolution. The resulting short pulse of UV light is detected by a phototube and lock-in amplifier. The polarization of the exciting light is varied by the half-wave plate permitting examination of $I_\parallel(t)$ and $I_\perp(t)$.

The experimental results reported in section V were obtained with a different experimental system. A 640-nm single pulse was obtained from the synchronously pumped dye laser described above. This pulse was frequency doubled to 320 nm and used for sample excitation. The resulting fluorescence was focused into a monochromator with a polarizer on the entrance slit and a Hamamatsu R1645U-01 microchannel plate attached to the exit slit (emission wavelength = 337 nm). A Tektronix R7912 transient waveform recorder digitized the signal from the microchannel plate and transferred the data to a minicomputer. The excitation polarization was varied with a half-wave plate, allowing either $I_\parallel(t)$ or $I_\perp(t)$ to be obtained. The detection system has a time response of 1 ns.

IV. Micelles

In this section we discuss picosecond fluorescence mixing experiments on excitation transfer among donors randomly distributed at the surface of Triton X-100 micelles.[26] Micelles have been extensively studied and their physical properties are relatively well understood. As such, they present a good physical situation for testing energy transport theories for finite volumes.

The donor chromophore used in these experiments is octadecyl rhodamine B (ODRB). The long hydrocarbon tail of ODRB increases the solubility of the chromophore in the micelle to such an extent that virtually every ODRB molecule is associated with a micelle. The micelle concentrations are sufficiently low that excitation transport between chromophores in different micelles is negligible. The charged nature of the chromophore assures that it is located at the micelle surface. Thus we can describe our experimental system by considering donor–donor energy transport on a sphere surface.

We calculated $G^s(t)$, the probability that the excitation is on

(31) J. A. Manson and L. H. Sperling, "Polymer Blends and Composites", Plenum, New York, 1976, p 77*ff*.
(32) D. A. McQuarrie, "Statistical Mechanics", Harper and Row, New York, 1976, p 256.
(33) M. D. Galanin, *Tr. Fiz. Inst. I. P. Pavlova*, **5**, 341 (1950).
(34) A. Jabloński, *Acta Phys. Pol. A*, **38**, 453 (1970).

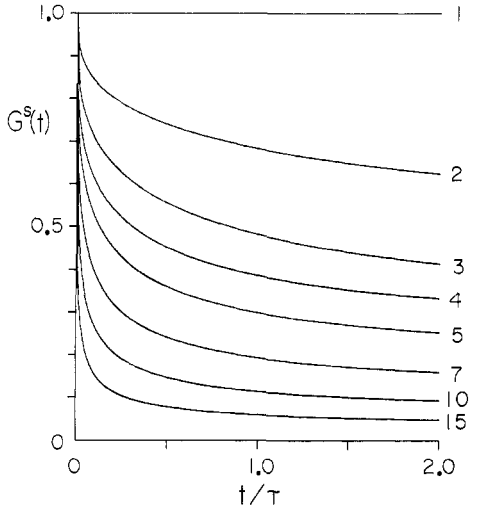

Figure 2. $G^s(t)$, the probability that the excitation is on the originally excited molecule, for 1–15 donor chromophores randomly distributed on a sphere of radius 37 Å. This value of the radius is used for the calculated curves in Figures 3 and 4. As the number of donors increases on a sphere of constant size, $G^s(t)$ decays faster. Time is in units of τ, the excited-state lifetime. (Note that $G^s(t)$ does not include lifetime decay. The curve for one donor, since there is no energy transport, has $G^s(t) = 1$ for all times.)

the originally excited molecule, for transport on a spherical surface using eq 7. In Figure 2, we show the results of this calculation for different numbers of chromophores randomly distributed on a sphere of radius $R = 37$ Å. (This value of the radius is the best fit to the experimental data presented below.) R_0 for ODRB was measured spectroscopically[1] to be 51.5 Å, and this value was used in the calculation. As the number of chromophores increases, energy transport becomes very efficient.

For ODRB in Triton X-100 micelles, the relationship between $G^s(t)$ and the fluorescence decays parallel and perpendicular to the excitation polarization is given by

$$I_{\parallel}(t) = e^{-t/\tau}(1 + 2C\phi(t)) \tag{8}$$

$$I_{\parallel}(t) = e^{-t/\tau}(1 - C\phi(t)) \tag{9}$$

where C is a constant ≤ 0.4 which describes the degree of photoselection for the transition involved. $\phi(t)$ contains all sources of depolarization. Since the ODRB chromophores rotate slowly within the micelle, $\phi(t)$ contains a small contribution due to molecular rotation[35] as well as energy transport.

$$\phi(t) = e^{-t/\tau_R}\sum_{n=0}^{\infty}\frac{N}{\mu}\left(\frac{e^{-\mu}\mu^N}{N!}\right)G^s(N,R,t) \tag{10}$$

In this expression, τ_R is the rotational lifetime and μ is the average number of chromophores per micelle. A Poisson distribution is employed to describe the distribution of ODRB among the micelles.

Fluorescence mixing experiments were performed as described in section III. First, a micelle solution where the ODRB concentration was so low that no energy transport could occur was examined. This allowed all parameters in eq 8–10 to be determined except the micelle radius. We next examined four solutions of successively higher chromophore concentrations (the Triton X-100 concentration was held fixed). The only parameter that we adjusted to account for the energy transport in this data was the micelle radius. The best fit to the data was obtained with $R = 37$ Å.

(35) R. S. Moog, M. D. Ediger, S. G. Boxer, and M. D. Fayer, *J. Phys. Chem.*, **86**, 4694 (1982).

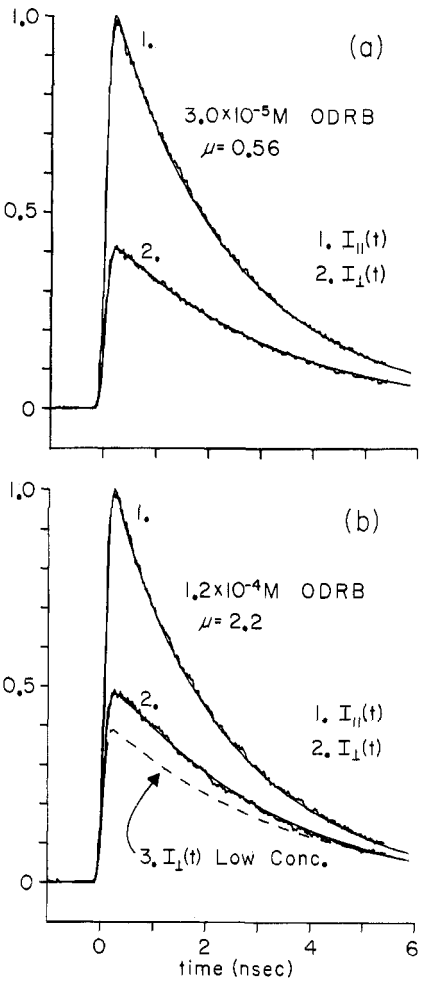

Figure 3. Time-resolved fluorescence intensity for (a) 3.0×10^{-5} M ODRB and (b) 1.2×10^{-4} ODRB in aqueous 0.5% Triton. The average number of chromophores per micelle $\pm = 0.56$ and 2.2, respectively. For each concentration, the fluorescence polarized parallel ($I_{\parallel}$) and perpendicular ($I_{\perp}$) to the polarization of the excitation light is shown. The smooth curves running through the data were calculated with eq 8 and 9. The only adjustable parameter, the micelle radius, has been fixed at 37 Å for all the calculated curves in this paper. In (b), we have shown as a dashed line $I_{\perp}(t)$ in the absence of energy transport. This comparison demonstrates that energy transport is already significant at $\mu = 2.2$. Note that the theory accurately predicts not only the shape of the experimental data but the relative heights of the two polarization components as well.

Figures 3 and 4 show the polarized fluorescence decays, as well as the smooth theoretical curves calculated with $R = 37$ Å. It is clear that the theory not only accurately predicts the *shapes* of $I_{\parallel}(t)$ and $I_{\perp}(t)$ but also the relative *heights*. In Figure 3b we have reproduced the low concentration $I_{\perp}(t)$ to illustrate that energy transfer is significantly affecting the experimental observable, even when the average number of chromophores per micelle is only 2.2. At higher concentrations (Figure 4), there is a slight discrepancy between the theoretical predictions and the experimental curves. These small deviations are explained by trapping by aggregates[3] of ODRB within the micelles.

Three main conclusions emerge from this work. (1) The statistical mechanical theory,[23] which employs a density expansion with a Padé approximant, provides a very good description of these finite volume systems. Energy transport theories developed for infinite volumes cannot explain the experimental results. (2) The efficiency of energy transport among donors is greatly enhanced by clustering the donors in the small volume micelle systems. (3) The energy transport measurements yield the radius of the micelles. The radius determined by these experiments is in good agreement with those measured by other techniques.[36,37] When

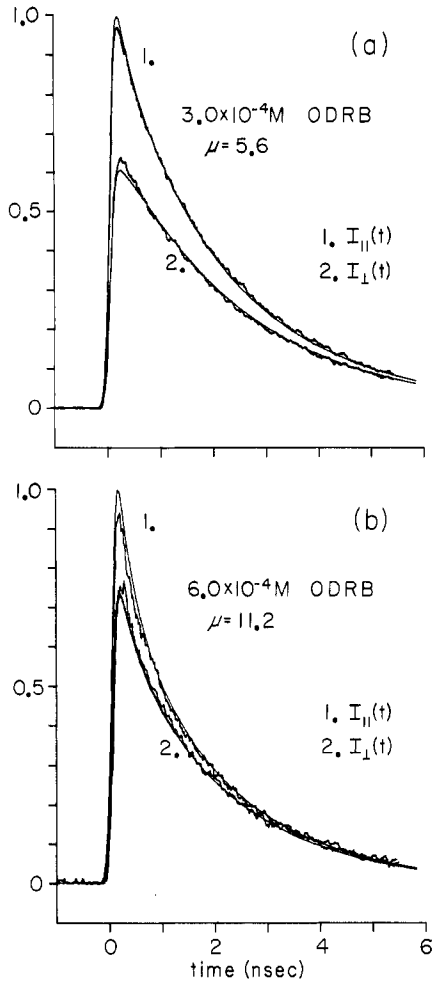

Figure 4. Time-resolved fluorescence mixing data for (a) 3.0×10^{-4} M ODRB and (b) 6.0×10^{-4} M ODRB in aqueous 0.5% Triton. The average number of chromophores per micelle $\mu = 5.6$ and 11.2, respectively. The smooth curves were calculated with eq 8 and 9. The micelle radius has been fixed at 37 Å. At these high concentrations, energy transport is rapid as indicated by the small difference between $I_{\parallel}(t)$ and $I_{\perp}(t)$. The slight discrepancies between the data and the calculated curves at these high concentrations are due to trapping by aggregates.

appropriate finite volume transport theories are utilized, energy transport experiments can provide quantitative information about the spatial extent of chromophore distributions.

V. Polymers

An isolated polymer coil provides another example of a finite volume energy transport system.[25] Excitation transport among coil chromophores depends both on local molecular structure and on thermodynamic interactions of the coil with its environment.[22] If an individual coil with a small fraction of chromophores is dissolved in a good solvent, it will assume an extended configuration. Because of the large average interchromophore separation, energy transport will be slow. If the polymer–solvent interactions are less favorable, the isolated coil will contract and excitation transport will become more probable. Because of their sensitivity to the spatial separation and orientation of chromophores in a polymer system, excitation transport observables contain detailed information about structural properties, e.g., coil configuration and the degree of coil extension.[19,25] This information is of key importance in understanding the microscopic interaction of a polymer with its environment, and thus the macroscopic properties of polymers and polymer blends.

Questions about coil dimensions and aggregation of coils are extremely difficult to address with current techniques when the polymer concentration is very small. This is particularly true of polymer blends, when a low concentration of guest polymer is mixed with another polymer. $G^s(t)$, because it can be obtained from time-resolved polarized fluorescence data,[17824] can be measured even at very low concentrations. $G^s(t)$ depends strongly on the degree of extension of a single polymer coil. As the solvent–polymer interactions are made less favorable, the coil will contract and $G^s(t)$ will decay faster due to the increased local concentration of chromophores attached to remote segments of the chain. $G^s(t)$ will also be sensitive to aggregation of polymer coils, either because of an increased chromophore density or, if the chromophore density does not increase, because of the larger volume of sites that the excitation can visit (increasing the finite volume).[25] Thus the observation of energy transport allows questions pertaining to the physical properties of isolated coils or small aggregates in various environments to be addressed.

The finite volume theory[23] outlined above can be used to calculate $G^s(t)$ for isolated polymer coils if a few modifications[25] are made. First, we restrict the application of the theory to polymers which contain only a small fraction of chromophore-containing monomers. This assures that the chromophore distribution about the originally excited chromophore is essentially three-dimensional. Second, we assume the model of chromophores randomly distributed in a sphere of radius R_s to be an approximate description of the subset of all coils with configurations having a particular radius of gyration R_g. (Thus, Ω in eq 6 and 7 is a spherical volume of radius R_s.) Associated with this distribution of chromophores is a second moment, i.e., the radius of gyration squared ($R_g^2 = (3/5)R_s^2$). By averaging $G^s(t)$ obtained for a particular R_g over a distribution function for R_g, $P(R_g)$, we obtain the ensemble averaged observable:

$$\langle G^s(N,\langle R_g^2\rangle,t)\rangle = \int_0^\infty dR_g\, P(R_g)\, G^s(N,R_g,t) \qquad (11)$$

For the purpose of illustrating this calculation below, the Flory–Fisk distribution function[38] was used for $P(R_g)$.

The energy transport calculation described above involves an average over a chromophore distribution with a sharp cutoff. The validity of this averaging procedure can be tested by calculating the ensemble average segmental distribution function implicit in this approach. Figure 5 shows the comparison of this distribution (dashed line) to the widely used Gaussian distribution function[39] (solid line). The agreement is very reasonable and demonstrates that our model is consistent with a Gaussian ensemble average density distribution.

Figure 6 shows how $G^s(t)$ is affected by changes in coil dimensions and by coil aggregation for a specific copolymer in blends with various hosts. For the purposes of illustration, parameters appropriate for a 20000 MW copolymer of vinylnaphthalene and methyl methacrylate (mole fraction of vinylnaphthalene = 0.15) have been used. R_0 is taken to be 13.0 Å, the same as for 2-ethylnaphthalene.[24] Curve A shows $G^s(t)$ calculated for the copolymer under Θ conditions ($\langle R_g^2\rangle^{1/2} = 37$ Å). Θ conditions imply that polymer–host interactions exactly cancel polymer excluded volume effects, hence random flight statistics are applicable.[39]

Curve B shows $G^s(t)$ for the same isolated polymer coil as it might appear at very low concentration in a polymer blend when the thermodynamic interactions between the host and guest polymers are unfavorable. The segmental density of the guest copolymer has been doubled at the center of the coil by decreasing $\langle R_g^2\rangle^{1/2}$ to 29 Å. The Flory–Fisk distribution was again used to describe the distribution of the radius of gyration. Curve B could be readily distinguished from curve A by, for example, time-resolved fluorescence depolarization measurements.

Curve C shows the change in $G^s(t)$ that would be expected upon

(36) Mario Corti and Vittorio Degiorgio, *Opt. Commun.*, **14**, 358 (1975).
(37) H. Hasko Paradies, *J. Phys. Chem.*, **84**, 599 (1980).
(38) P. J. Flory and S. Fisk, *J. Chem. Phys.*, **44**, 2243 (1966).
(39) Kiromi Yamakawa, "Modern Theory of Polymer Solutions", Harper and Row, New York, 1971.

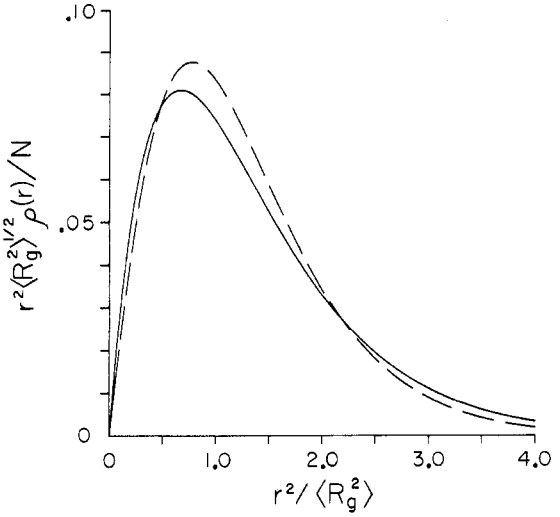

Figure 5. Comparison of the standard Gaussian ensemble average segmental density distribution (solid line) to the density distribution implicit in the polymer excitation transport calculations (dashed line). Note that these are radial distribution functions.

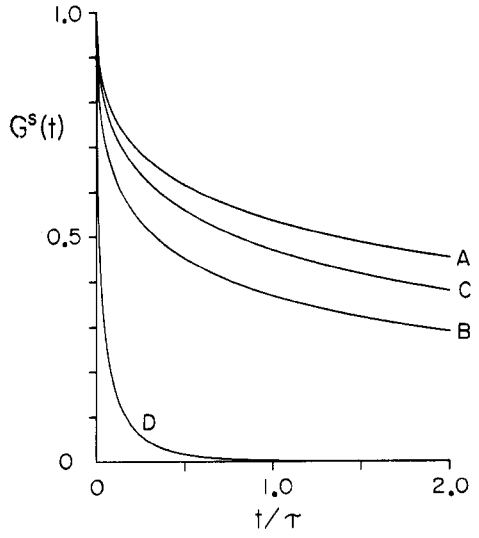

Figure 6. The calculated effects of density changes and aggregation on $G^s(t)$ for a 20 000 MW copolymer of methyl methacrylate and vinylnaphthalene (mole fraction of vinylnaphthalene = 0.15). Curve A shows a calculation for an ensemble of coils under Θ conditions ($\langle R_g^2\rangle^{1/2}$ = 37 Å). Each coil contains 28 chromophores. Curve B shows the same copolymer when the coils have contracted due to unfavorable interactions with the host polymer ($\langle R_g^2\rangle^{1/2}$ = 29 Å). Curve C shows an aggregate of 16 coils, assuming that the average density is the same as under Θ conditions and that the Flory–Fisk distribution of the radius of gyration can be applied to the aggregate. This is the minimum change that could be expected upon aggregation. For C, there are 448 chromophores with $\langle R_g^2\rangle^{1/2}$ = 93 Å. Curve D shows an infinite volume calculation for a bulk sample of the pure copolymer (1 g/cm³).

aggregation of single coils if the average chromophore density of the coils is the same as in curve A (Θ conditions). In this case only the volume accessible to the excitation (i.e., the numer of sites) increases. This is clearly the minimum change that would be expected upon aggregation. If the chromophore density increased as well, the difference between curves A and C would be greater. For comparison, curve D shows an infinite volume calculation (using the theory of Gochanour, Andersen, and Fayer[15]) for conditions corresponding to a macroscopic volume of the pure copolymer.

In Figure 7, the results of a time-resolved fluorescence depolarization experiment[24] are compared to the theory presented in this section. The sample is a 20 000 MW copolymer of 2-

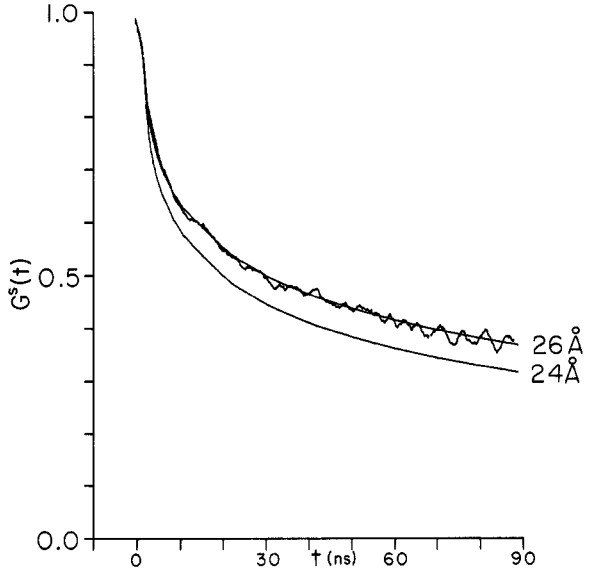

Figure 7. $G^s(t)$ for isolated coils of a 20 000 MW copolymer of methyl methacrylate and 2-vinylnaphthalene in a PMMA host. The smooth curve running through the data is a theoretical calculation using eq 11 and the appropriate convolution with the detection system's impulse response function. The theoretical curve was obtained by varying a single parameter, $\langle R_g^2\rangle^{1/2}$, to give the best fit to the experimental data. This value, 26 Å, is close to that expected for a 20 000 MW PMMA homopolymer under Θ conditions. A second curve with $\langle R_g^2\rangle^{1/2}$ = 24 Å indicates the sensitivity of the observable to the polymer size.

vinylnaphthalene and methyl methacrylate (mole fraction of vinylnaphthalene = 0.10). The host material is 120 000 MW poly(methyl methacrylate) (PMMA). The copolymer concentration in successive PMMA samples was lowered until no further changes in the fluorescence depolarization were detected (3/8 wt %). Thus, the experimental $G^s(t)$ curve in Figure 7 is characteristic of excitation transport among the chromophores of the isolated copolymer coil; excitation transport to chromophores on other chains is negligible.

The experimental $G^s(t)$ curve was obtained as follows: First, the fluorescence anisotropy, $r(t)$

$$r(t) = \frac{I_\parallel(t) - I_\perp(t)}{I_\parallel(t) + 2I_\perp(t)} \tag{12}$$

was calculated from the polarized fluorescence data. Then fluorescence depolarization data were collected for a second copolymer, one in which the 2-vinylnaphthalene mole fraction is so low that excitation transport can be neglected. The fluorescence anisotropy calculated from this data contains a very small amount of depolarization due to motion of the chromophores. The experimental $G^s(t)$ is obtained by taking the ratio of the fluorescence anistropies of the two copolymers.[24] This procedure removes the depolarization due to molecular motion.

The theoretical curve shown in Figure 7 which passes through the data was obtained by convolving $I_\parallel(t)$ and $I_\perp(t)$ with the impulse response function and using eq 12 to calculate $G^s(t)$. A single parameter, $\langle R_g^2\rangle^{1/2}$, was adjusted to obtain the best fit. The curve shown has $\langle R_g^2\rangle^{1/2}$ = 26 Å. To indicate the sensitivity of the observable to $\langle R_g^2\rangle^{1/2}$, a second curve with $\langle R_g^2\rangle^{1/2}$ = 24 Å is shown. The accepted value[40] for a 20 000 MW PMMA homopolymer is 37 ± 4 Å.

The reason for this discrepancy is that the pair correlation function implicit in the theory is not appropriate for a 20 000 MW PMMA chain. When the correct pair correlation function is

(40) M. Jurata, Y. Tsunashima, M. Iuama, and K. Kamada in "Polymer Handbook", J. Bradrup and E. H. Immergut, Ed., Wiley-Interscience, New York, 1975, p IV-38.

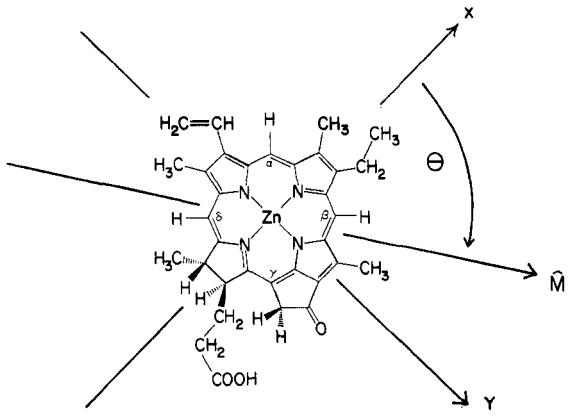

Figure 8. Structure of zinc pyrochlorophyllide a molecule. By convention, the coordinate system of x and y in-plane axes is as depicted. $\hat{M}$ denotes the unit vector of the transition dipole moment for the lowest excited singlet state. θ is the angle $\hat{M}$ makes with the x axis.

considered, the theoretical fit yields a $\langle R_g^2 \rangle^{1/2}$ which lies within the error bars of the accepted value.[24] The fact that the theory predicts the correct shape for $G^s(t)$ and yields a $\langle R_g^2 \rangle^{1/2}$ value close to that of the Θ condition homopolymer demonstrates that essential aspects of polymer statistics have been incorporated.

Experiments are presently being conducted in our laboratory on isolated polymer coils in a variety of host materials and on phase-separated blends. The above discussion makes clear the possibility of obtaining new insights into the microscopic interactions of polymers in the solid state.

VI. Chlorophyll Transition Dipole Moment Orientation

In the systems described above, the observation of energy transport was combined with the knowledge or measurement of molecular parameters to extract information about the spatial distribution of chromophores.[25,26] In this section, we describe an experimental system where the knowledge of the spatial position and orientation of the chromophores allows the extraction of a molecular property.[29] The property of interest is the orientation of the transition dipole within the chlorophyll molecule. This quantity is significant for the interpretation of experiments on natural chlorophyll-containing systems, and for our understanding of the molecular architecture of these systems.

Figure 8 shows the zinc pyrochlorophyllide a molecule and specifies the orientation of the transition dipole in terms of the angle θ. In order to determine θ, two chloropfhyllide molecules have been substitutionally incorporated into a host protein (hemoglobin).[29,41] Proteins possess specific binding sites for their chromophores. The reconstitution of human semihemoglobins with two chlorophyllides takes advantage of this aspect of protein structure, providing a system of two chromophores separted by a sufficient distance so that exchange and excitonic interactions are absent.[42] The well-defined tertiary and quaternary structure of the hemoglobin molecule ensures that the relative orientation of each interacting pair of chlorophyllides is constant.

The protein α^h(deoxy)β^{Chl} (hemoglobin with the heme in each β chain replaced by chlorophyllides, and the α chain hemes in the deoxy state) possesses an interchlorophyllide center-to-center separation of 40.2 Å. The exact value of the transfer rate constant is dependent on the mutual orientation of the two transition dipoles (K_{jk}, in eq 2), as well as this distance.[1] Because the interchromophore separation is known and R_0 can be measured independently,[1,29] the measurement of the transfer rate constant allows the orientation of the transition dipole to be established.

Fluorescence mixing experiments were performed on the system described above.[29] The fluorescence anisotropy, $r(t)$, was calculated from experimental observations at discrete times (see eq 12).

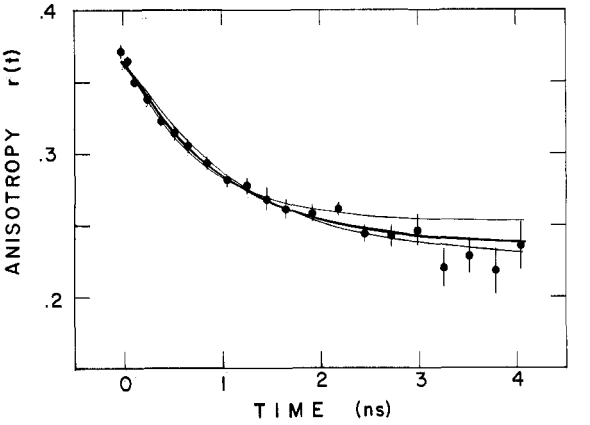

Figure 9. Fluorescence anisotropy of α^h(deoxy)β^{Chl}. The dots represent the data and are the average of three to seven anisotropy determinations. The error bars are standard deviations of the mean. The solid curves cover the range of chlorophyll transition dipole directions which provide fits to the data and yield a value of $\theta = 95 \pm 2°$.

At the moment of the exciting pulse, only originally photoselected chromophores fluoresce and the emission anisotropy is at its maximum value, the monomer anisotropy (r_0). The anisotropy then degrades in time by an exponential decay governed by the rate (w_{12}) of the intraprotein excited-state population transfer to the other, originally unexcited, chromophore. At a time sufficiently long so that the excited-state population has equilibrated between the two chlorophyllides, a characteristic nonzero emission anisotropy, r_∞, is observed. Both r_∞ and w_{12} contain information about the relative orientation of the lowest energy singlet transition dipole moment.

The results of the time-resolved measurements are presented in Figure 9. Each data point is the average of three to seven anisotropy determinations. The error bars represent corresponding standard deviations. The anisotropy decay has the form of an exponential decay to a nonzero baseline, as anticipated for this system. The smooth curves are theoretical fits for the small range of possible orientations of the transition dipole which fits the data.

The combination of this time-resolved data and steady-state fluorescence anisotropy data[29,42] allowed the orientation of the transition dipole to be fixed, with $\theta = 95 \pm 2°$. This value falls within the range of values calculated theoretically[43-45] and will be of considerable importance in furthering our understanding of chlorophyll-containing systems in nature.

VII. Concluding Remarks

In this article, we have reviewed recent experimental and theoretical progress in the study of electronic excited-state transport processes in disordered finite volume systems. The experiments on micelles demonstrate that clustered transport systems can provide extremely efficient excitation transport even at low bulk concentrations. In analogy to natural photosynthetic units, these clustered systems may be useful in a solar energy conversion scheme. The micelle experiments also demonstrate that the size of a small system can be determined by properly analyzing excitation transport data in terms of a finite volume theory. The application of this idea to polymer systems will allow detailed information about microscopic interactions in polymer blends to be obtained. These interactions are of critical importance because they determine bulk properties of the composite material. The determination of the chlorophyll transition dipole direction illustrates that an important intrinsic molecular property can be obtained from a carefully designed excitation transport experiment.

For many years scientists have recognized that electronic ex-

(41) K. A. Wright and S. G. Boxer, *Biochemistry*, **20**, 7546 (1981).
(42) A. Kuki and S. G. Boxer, *Biochemistry*, **22**, 2923 (1983).
(43) J. C. Chang, *J. Chem. Phys.*, **67**, 3901 (1977).
(44) J. D. Petke, G. M. Maggiora, L. L. Shipman, and R. E. Christofferson, *Photochem. Photobiol.*, **30**, 203 (1979).
(45) C. Weiss, *J. Mol. Spectrosc.*, **44**, 37 (1972).

cited-state transport processes provide detailed information about intermolecular interactions in condensed phases. The experiments discussed in this paper illustrate the additional utility of excitation transport for the investigation of molecular properties and the properties of large assemblies of molecules.

Acknowledgment. The work described here involved the efforts of a number of individuals at Stanford and we take this opportunity to acknowledge them. R. P. Domingue and K. A. Peterson collaborated on the finite volume excitation transport experiments, and Dr. Richard S. Moog, Atsuo Kuki, and Professor Steven G. Boxer collaborated on the chlorophyll experiments. This work was made possible by financial support from the Department of Energy, Office of Basic Energy Sciences (Grant No. DE-FG03-84ER13251), and the National Science Foundation, Division of Materials Research (Grant No. DMR 79-20380). In addition, the National Science Foundation Stanford Center for Materials Research contributed to the support of this research. M.D.F. acknowledges the Simon Guggenheim Memorial Foundation for Fellowship support which contributed to this research.